Kirsi Lauerma, MD
Pekka Niemi, MD
Helena Hänninen, MD
Tuula Janatuinen, MD
Liisa-Marja Voipio-Pulkki, MD
Juhani Knuuti, MD
Lauri Toivonen, MD
Timo Mäkelä, MSc
Markku A. Mäkijärvi, MD
Hannu J. Aronen, MD

Index terms:
Coronary angiography, comparative studies, 54.1244
Coronary vessels, stenosis or obstruction, 54.76
Magnetic resonance (MR), cine study, 524.12144
Magnetic resonance (MR), comparative studies, 524.121412, 524.121413, 524.12143, 524.12144
Magnetic resonance (MR), contrast enhancement, 524.12143
Magnetic resonance (MR), inversion recovery, 524.121413
Myocardium, infarction, 511.711
Myocardium, PET, 511.12163

Radiology 2000; 217:729–736

Abbreviation:
FDG = 2-[fluorine 18]fluoro-2-deoxy-D-glucose

[1] From the Depts of Radiology (K.L., P.N., H.J.A.), and Medicine, Division of Cardiology and BioMag Laboratory, (H.H., L.T, M.A.M.), Helsinki University Central Hospital (HUCH), Haartmaninkatu 4, 00029 Helsinki, Finland; Dept of Clinical Radiology, Kuopio University Hospital, Finland (H.J.A.); Turku PET Centre, Finland (T.J., L.M.V.P., J.K.); and Laboratory of Biomedical Engineering, Helsinki University of Technology, Finland (T.M.). From the 1999 RSNA scientific assembly. Received Nov 29, 1999; revision requested Jan 14, 2000; revision received Apr 3; accepted Apr 21. Supported by HUCH and Orion research funds, HUCH Foundation, Finnish Cardiac Society, Academy of Finland, and Paavo Nurmi Foundation, Helsinki, Finland. **Address correspondence to** K.L. (e-mail: *kirsi.lauerma@hus.fi*).

Author contributions:
Guarantors of integrity of entire study, K.L., P.N., H.H., H.J.A. The complete list of author contributions appears at the end of this article.

Multimodality MR Imaging Assessment of Myocardial Viability: Combination of First-Pass and Late Contrast Enhancement to Wall Motion Dynamics and Comparison with FDG PET—Initial Experience[1]

PURPOSE: To combine three magnetic resonance (MR) imaging modalities—dobutamine stress cine, first pass, and late contrast material–enhanced T1-weighted imaging—and to compare the results with 2-[fluorine 18]fluoro-2-deoxy-D-glucose (FDG) positron emission tomography (PET) in the assessment of unviable myocardium in coronary artery disease.

MATERIALS AND METHODS: Ten patients with multivessel coronary artery disease underwent MR imaging before and 6 months after bypass surgery. Left ventricular cine MR imaging was performed at rest and during dobutamine infusion. Inversion-recovery gradient-echo images were obtained to study myocardial contrast enhancement at first pass and 5 minutes later. FDG PET was performed with orally administered acipimox before surgery.

RESULTS: With dobutamine cine MR imaging, unviable myocardium was detected with a sensitivity of 79% and a specificity of 93%; postoperative wall thickening was the standard. First-pass analysis increased these values to 97% and 96%; analysis of late enhancement with T1-weighted imaging, to 62% and 98%. FDG PET had a sensitivity of 81% and a specificity of 86%.

CONCLUSION: The combination of first-pass enhancement analysis and wall motion assessment with stress significantly increases the specificity of MR imaging in the detection of unviable sectors.

Assessment of myocardial viability with a clinical magnetic resonance (MR) imager would increase the feasibility of MR imaging in coronary artery disease. Dobutamine stress cine imaging has been used for both ischemia induction (1) and viability assessment (2). Compared with echocardiography, MR imaging is more accurate in viability assessment because MR images can be acquired with reproducible quality independent of the examiner or patient anatomy (3). First-pass contrast enhancement with the use of T1-weighted fast sequences has shown promise in the detection of ischemia and infarction (4), especially when combined with pharmacologic stress and the administration of dipyridamole (5) or adenosine (6), which specifically increase coronary artery flow. Contrast enhancement on T1-weighted images of acutely infarcted myocardium in patients was reported in 1988 (7), but this phenomenon has not been used for clinical purposes. The combination of these techniques at one MR imaging session has been tested in only a few recent studies (8–10).

The purpose of our study was to determine the effect of the addition of information

from first-pass MR imaging and from late enhancement on T1-weighted images to dobutamine stress cine imaging. We compared MR imaging results to those obtained with 2-[fluorine 18]fluoro-2-deoxy-D-glucose (FDG) positron emission tomography (PET), a method that has been shown to depict unviable myocardium with great accuracy (11). Left ventricular wall thickening was assessed with MR imaging 6 months after bypass surgery, and the findings of wall thickening at rest were used as the standard.

MATERIALS AND METHODS

Study Protocol

The study protocol was approved by the local ethics committee. Ten consecutive patients with multivessel coronary artery disease and regional wall motion abnormality depicted at angiography and with need of revascularization were included. FDG PET and MR imaging were performed within 10 days. All patients underwent bypass surgery after imaging. Six months after surgery, MR imaging was repeated for assessment of myocardial response to revascularization.

Patients

Informed consent was obtained from all patients before they entered the study. The mean age of the patients was 69 years (range, 64–71 years); eight were men, two were women. Four patients belonged to group III, five to group II, and one to group I according to the New York Heart Association functional classification. Seven patients had a history of myocardial infarction, and the mean time from last infarction to MR imaging was 16 months (range, 3–60 months). In addition to coronary artery disease, patients had diabetes ($n = 3$), hypertension ($n = 2$), psoriasis ($n = 2$), and/or hypercholesterolemia ($n = 1$).

Coronary Angiography and Interpretation of Findings

Coronary angiography was performed with 6-F catheters and imaging in multiple projections. Iobitrol (Xenetix; Guerbet, Aulnay-Sous-Bois, France) with 350 mg of iodine per milliliter was used as the intraarterial contrast material. Left ventricular cine angiograms were obtained in the 30° right anterior oblique projection. The images were interpreted by an experienced angiographer (L.T.). The level and degree of stenosis in the main branches of the coronary arteries were visually estimated, and reduction in coronary artery diameter of more than 70% was considered significant. The presence of dyskinetic anatomic regions was estimated from left ventricular cine angiograms.

MR Imaging Protocol

Combined MR imaging was performed in all patients before and 6 months after multivascular bypass surgery. An 18-gauge catheter was inserted into the antecubital vein for dobutamine (Dobuject; Leiras, Helsinki, Finland) infusion and gadopentetate dimeglumine (Magnevist; Schering, Helsinki, Finland) injection. Patients were positioned supine on the table of a 1.5-T imager (Magnetom Vision; Siemens, Erlangen, Germany), and imaging was performed with the body array coil as a receiver. Transverse, oblique sagittal, and double-oblique left ventricular long-axis scout images were obtained to determine the final short-axis imaging plane. A left ventricular short-axis orientation was selected for MR imaging to minimize partial volume effects and to enable comparison between myocardial regions perfused by different arteries and between MR imaging and PET findings.

Blood pressure was monitored before and during dobutamine infusion, and continuous heart rate monitoring was performed during MR imaging. In addition, two-way audio communication and video monitoring of the patient were maintained.

Regional systolic wall thickening was monitored with an electrocardiographically gated breath-hold cine sequence. The imaging parameters for the series were as follows: repetition time msec/echo time msec, 40/4.8; matrix, 126 × 256; field of view, 240 × 320 mm; and section thickness, 8 mm. Five short-axis sections 15 mm apart were imaged at rest, and three of these with regional hypokinesia were imaged during dobutamine infusion of 5 μg per kilogram of body weight per minute.

To monitor the first transit of bolus injection of contrast agent during dobutamine infusion, electrocardiographically gated, inversion-recovery gradient-echo images were acquired in the same three left ventricular short-axis planes with the following parameters: 3.3/1.4; matrix, 62 × 128; field of view, 240 × 320 mm; section thickness, 10 mm; and flip angle, 8°. An inversion time of 400 msec was selected to nullify the myocardial signal before contrast material administration. Perfused with gadopentetate dimeglumine, the myocardium would show relatively increased signal intensity because of the predominant T1 shortening.

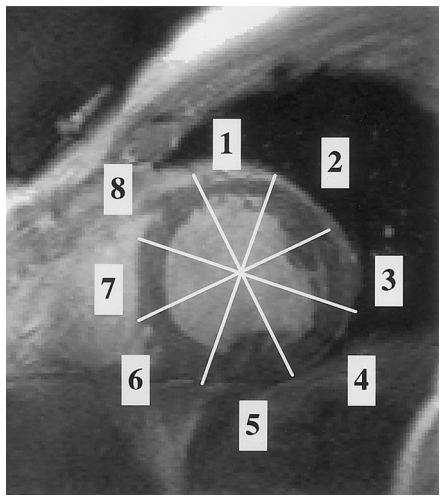

Figure 1. Anatomic basis for MR imaging and PET image analysis. Left ventricular short-axis MR images were divided into eight sectors (*1–8*) in a clockwise fashion by using the interventricular groove as the starting point. On the MR images, systolic wall thickening at rest and with stress, first-pass enhancement, and late enhancement on T1-weighted images were measured in each sector. On PET images, the FDG uptake was determined in corresponding sectors.

Sets of 60 images were acquired, with the three sections imaged repeatedly. Each set of images in the three sections was obtained every four to six R-R intervals (approximately 4 seconds), and one inversion-recovery preparation pulse was followed by an imaging sequence for a single section. After the third set of the three sections, gadopentetate dimeglumine (0.05 mmol/kg) was injected intravenously with a rate of 5 mL/sec.

After the first-pass study, dobutamine infusion was discontinued, and 5 minutes later, inversion-recovery gradient-echo images were obtained. Increased signal intensity would be a sign of increased extracellular volume, as in myocardial infarction.

MR Image Analysis

In each patient, the three left ventricular short-axis sections were divided into eight 45° sectors from the interventricular groove in a clockwise fashion (Fig 1). These sectors were analyzed for systolic wall thickening, first-pass enhancement, and late enhancement with NIH IMAGE 1.59 (Bethesda, Md; available at *rsb.info.nih.gov/nih-image*), an image analysis program. One author (K.L.) performed the analysis of each MR modality (enhancement on cine, first-pass, and late T1-

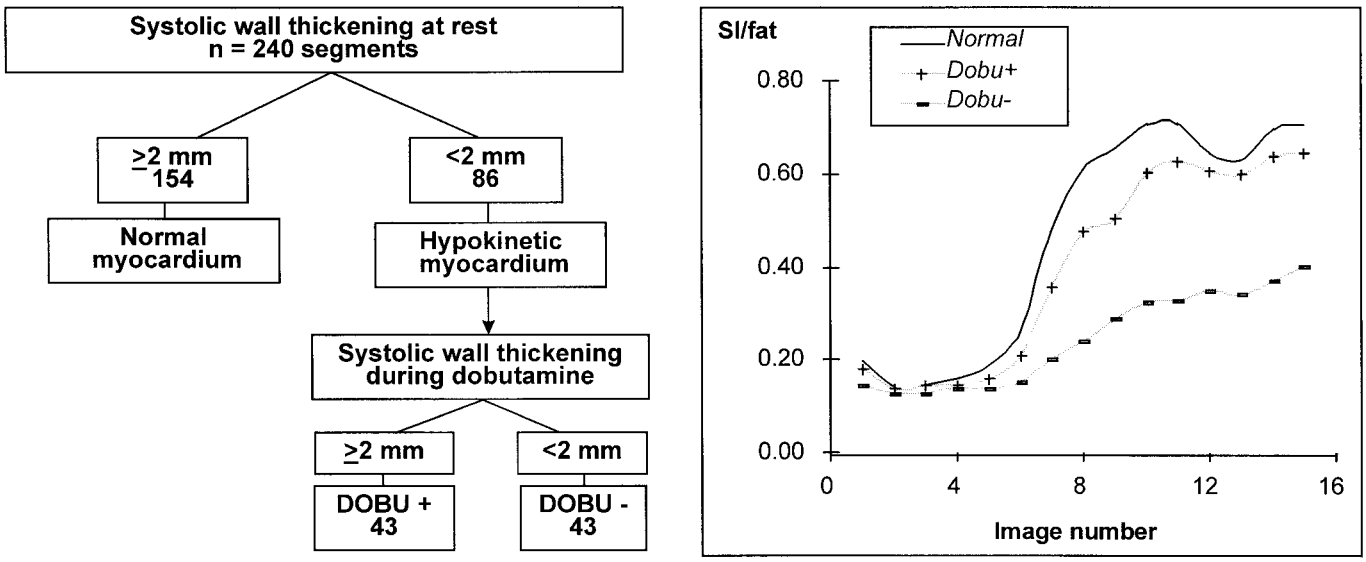

a. b.

Figure 2. Assessment of **(a)** sectional left ventricular systolic wall thickening and **(b)** first-pass enhancement. Sectors (n = 240) were divided into three groups: normal myocardium (wall thickening ≥ 2 mm at rest), *Dobu+* group (wall thickening < 2 mm at rest but ≥ 2 mm during dobutamine infusion), and *Dobu−* group (wall thickening < 2 mm at rest and no response to dobutamine). **(b)** Mean signal intensity–time curves of 43 sectors in each group. Fastest enhancement was observed in normal sectors, and clear hypoperfusion was shown in *Dobu−* sectors. The intensity curve of *Dobu−* sectors differs significantly ($P < .05$) from normal and *Dobu+* curves when tested by using analysis of variance with repeated measures. *SI* = signal intensity.

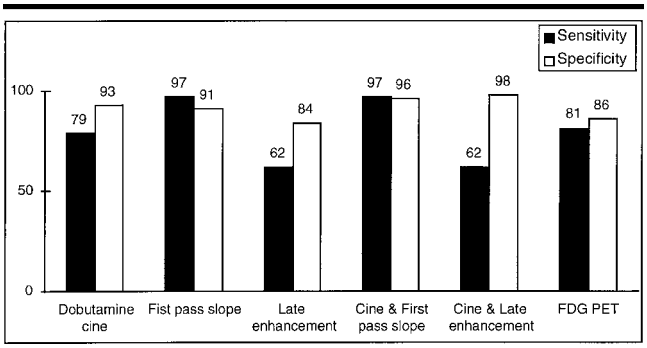

Figure 3. Sensitivity and specificity of single and combined MR imaging modalities in the detection of unviable myocardium in patients with regional left ventricular hypokinesia and comparison with FDG PET. Numbers are percentages.

weighted contrast-enhanced images) separately and was blinded to the rest of the results.

Left Ventricular Systolic Wall Thickening

Diastolic wall thickness for each sector was measured from the first image of the cine sequence; and systolic wall thickness, from the image with the smallest left ventricular chamber volume. Systolic wall thickening was calculated from these values. Sectors were divided into three groups according to systolic wall thickening at rest and during dobutamine infusion, as shown in Figure 2. Sectors with systolic wall thickening of least 2 mm at rest were considered normal (12). Sectors with systolic wall thickening of less than 2 mm at rest were classified to Dobu+ and Dobu− groups, depending on their response to dobutamine infusion. During infusion, Dobu+ sectors had systolic wall thickening of at least 2 mm; and Dobu− sectors, of less than 2 mm. The hypokinetic sectors (systolic wall thickening < 2 mm) that responded to bypass surgery (systolic wall thickening ≥ 2 mm at rest) were classified as hibernating, and those that did not were classified as unviable.

First-Pass Enhancement

The effect of gadopentetate dimeglumine injection was quantified by measuring signal intensity changes in left ventricular chamber blood, the eight myocardial sectors on each imaged section, and subcutaneous fat. The size (40 mm^2 ± 13 [SD]; range, 24–71 mm^2) and shape of the irregular myocardial regions of interest were kept constant throughout the analysis of each sector, but the sectors were individually traced from image to image because of breathing motion. Signal intensity–time curves were generated for regional first-pass enhancement analysis (Fig 2). The rate of increase in signal intensity in the myocardial sectors was assessed from the upslope of signal intensity–time curves of each perfusion study and was calculated with the equation slope = signal intensity increase/time, as described previously (5).

Late Enhancement on T1-weighted Images

The last T1-weighted inversion-recovery gradient-echo images that were obtained 5 minutes after contrast injection were used for the late enhancement analysis. A circumferential 5-mm region of interest was drawn on the myocardium, and care was taken to avoid pixels in the blood pool or epicardial fat. The signal intensity profile was produced by plotting the mean

signal intensity of the three pixels against the angular position (13). The mean plus or minus the SD of signal intensity in the normal myocardium in the lower-intensity region was calculated for each section, and the sectors with a signal intensity of 2 SDs above the mean were classified to represent the areas with larger extracellular volume (Fig 3).

Left Ventricular Ejection Fraction

All left ventricular short-axis images were planimetered with a mouse-driven cursor, and left ventricular volumes were summed to give the total cavity volume at diastole and systole according to the Simpson rule algorithm.

FDG PET and Comparison with MR Imaging

All patients underwent FDG PET before bypass surgery (Fig 4). Acipimox (Olbetam, Stabilimento di Ascoli Piceno, Marino del Tronto, Italy; 250 mg) was orally administered to patients 3.0 and 1.5 hours before FDG was injected. Dynamic PET was performed for 60 minutes; the imaging procedure and analysis were described in detail previously (11). FDG was synthesized with an automatic apparatus by using a modified method of Hamacher et al (14). The patients were positioned supine on a 15-section tomograph (Ecat 931/08-12; Siemens/CTI, Knoxville, Tenn) with a measured axial resolution of 6.7 and 6.5 mm in plane, and 250 MBq ± 35 of FDG was injected intravenously over 30 seconds. Dynamic imaging of the thoracic region was started simultaneously and continued for 60 minutes.

All data were corrected for dead time, decay, and measured photon attenuation. The three myocardial short-axis sections that corresponded to the sections imaged with MR were selected by measuring their distance from left ventricular apex and were divided into eight sectors by one author (T.J.). The sectors were aligned by defining the anterior interventricular groove visible with both imaging methods. Fractional utilization constants of FDG(K^i) and rates of myocardial glucose utilization were calculated for each sector, and results were compared with viability results obtained from MR imaging. The cutoff value for viability was set to 80% of normal myocardium in the lateral left ventricular wall (11).

Statistical Analysis

All values were expressed as the mean plus or minus the SD. The significance of differences in signal intensity–time curves, slopes, and late enhancement of sector groups was determined by means of repeated analysis of variance, or ANOVA, measures with multiple comparison of mean values by using the Scheffe *f* test. Differences in left ventricular ejection fraction before and after surgery on MR cine images were tested with the paired Student *t* test. A significance level of less than 5% was used.

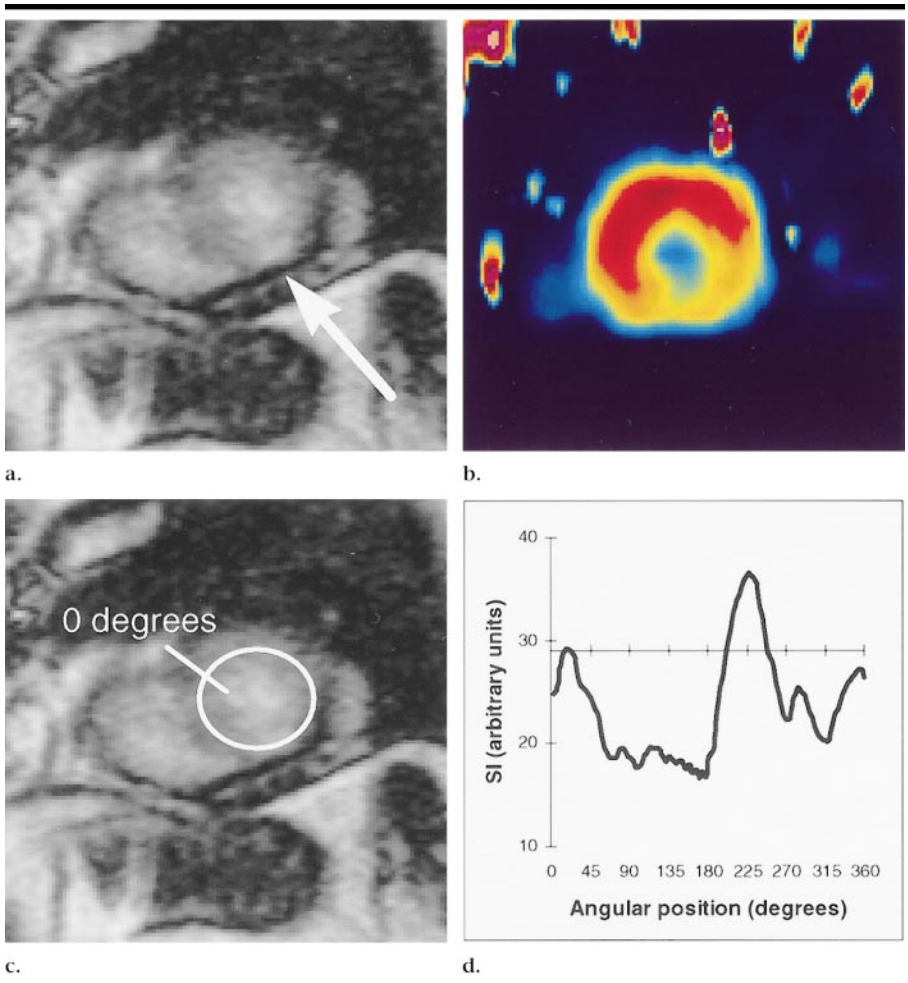

Figure 4. Assessment of late enhancement at T1-weighted imaging and comparison with FDG PET. **(a, c)** Contrast-enhanced T1-weighted MR images were obtained with an inversion-recovery gradient-echo sequence (repetition time msec/echo time msec/inversion time msec, 3.3/1.4/400; flip angle, 8°; section thickness, 10 mm; field of view, 240 × 320 mm; and matrix, 62 × 128.) **(a)** Image was obtained at the left ventricular short-axis apical level 5 minutes after gadopentetate dimeglumine injection. The arrow indicates the hyperintense zone in the posterior part of the left ventricular wall, which is a marker of larger extracellular volume and possible infarction. **(b)** FDG PET image shows decreased activity at the same site. **(c)** Circumferential region of interest was drawn on **a** from the interventricular groove clockwise to measure the signal intensity, site, and size of the hyperintense zone. **(d)** Plot of signal intensity (*SI*) in the circumferential region of interest versus the angular position on the left ventricular wall. The line at 29 arbitrary units indicates the cutoff value calculated as the signal intensity mean plus 2 SD from the value in normal myocardium, and the peak of the curve above it represents the hyperintense zone.

RESULTS

Coronary Angiography

At coronary angiography, all patients had at least 70% stenosis in two main coronary arteries and at least 50% stenosis in the third. On the right anterior oblique projection, all patients had regional dysfunction, six in the posterior wall and four in anterior wall. The mean ejection fraction was 46% ± 15 (range, 30%–80%).

MR Imaging

The mean left ventricular ejection fraction measured from short-axis cine sections increased from 44% before to 51% after surgery (ranges, 16%–62% before and 20%–69% after; $P < .004$). Systolic wall thickening at rest was normal (≥2

Anatomic Distribution of False-Positive and False-Negative Sectors in the MR Imaging Assessment of Unviable Myocardium

Location	Dobutamine Stress Cine		First-Pass Contrast-enhanced		Late Contrast-enhanced T1-weighted	
	False-Positive	False-Negative	False-Positive	False-Negative	False-Positive	False-Negative
Apex						
Anterior*	2	0	0	2	9	0
Lateral†	2	0	1	2	5	0
Posterior‡	2	1	0	3	4	2
Middle						
Anterior*	0	1	0	1	3	2
Lateral†	0	0	0	1	2	2
Posterior‡	2	1	0	4	1	1
Base						
Anterior*	2	0	0	2	6	1
Lateral†	0	1	0	0	3	1
Posterior‡	4	2	0	3	1	2

Note.—Data are the number of sectors. Findings at left ventricular cine MR imaging performed 6 months later were used for the standard.
* 89°–315°.
† 90°–224°.
‡ 225°–314°.

mm) in 154 sectors and hypokinetic (<2 mm) in 86 sectors (Fig 2a). Of the hypokinetic sectors, 43 responded to dobutamine infusion, and 43 did not. Six months after bypass surgery, 211 sectors had normal systolic wall thickening. Twenty-nine were still hypokinetic and were therefore labeled unviable. The 57 preoperatively hypokinetic sectors that had recovered after surgery were labeled hibernating. Figure 3 illustrates the high sensitivity and specificity of dobutamine cine and wall motion analysis (79% and 93%), as well as those of other MR modalities, for the detection of unviable sectors.

The six sectors with a response of at least 2 mm to dobutamine but with no recovery after surgery were observed in four different patients, and the 14 sectors with a response of less than 2 mm to dobutamine but with normal systolic wall thickening after surgery were observed in nine different patients. The majority of the false-positive and false-negative sectors were seen in the posterior left ventricular wall, as listed in the Table. Figure 5 illustrates the depiction of a posterior unviable sector, as confirmed at postoperative cine imaging and FDG PET, with all MR modalities.

First-pass enhancement curves of the sectors that did not respond to dobutamine were significantly lower that those of the sectors that did ($P = .03$) (Fig 2b). As shown in Figure 6a, the slope of the signal intensity–time curve [(intensity change/fat intensity)/seconds] was highest in sectors with normal systolic wall thickening and lowest in sectors with no response to dobutamine ($P < .002$). The range of slopes in normal, hibernating, and unviable sectors is illustrated in Figure 6b. There was only one unviable sector with a slope of more than 1.0. With a slope of 1 as the cutoff value, sensitivity and specificity in the detection of unviable sectors was 97% and 91% (Fig 3). The 18 viable sectors with slope of less than 1 were seen in seven patients (Table).

There were 52 sectors that had a signal intensity on contrast-enhanced T1-weighted images that was 2 SDs higher than that of normal myocardium. The mean relative signal intensity value in unviable sectors was significantly higher than that of hibernating or normal sectors ($P < .001$) (Fig 6c). The sensitivity and specificity of contrast enhancement on T1-weighted images in the detection of unviable myocardium were lower than those of other MR modalities (Fig 3). The majority of false-positive sectors were seen in the anterior left ventricular wall in all 10 patients, and false-negative sectors were seen in five patients (Table).

The combination of first-pass slope analysis and dobutamine cine systolic wall thickening assessment increased sensitivity and specificity to 97% and 96%, respectively, in the detection of unviable sectors. Late enhancement increased the specificity to 98% but decreased the sensitivity to 62% (Fig 3). In comparison, FDG PET in the same sectors had a sensitivity and specificity of 81% and 86%, respectively.

DISCUSSION

The question of myocardial viability in coronary artery disease can be answered with the use of scintigraphy and echo methods, but only with MR imaging can the combination of wall motion, perfusion, and tissue characteristics be assessed with good regional accuracy. Although authors of many review articles (15–17) recommend the use of cine MR imaging in combination with other MR techniques, to our knowledge only a few original reports (8,9) are available. We studied the effect of combining contrast-enhanced MR imaging sequences with low-dose dobutamine cine assessment.

The major finding of this study was the significantly higher first-pass enhancement slope in myocardial hypokinetic sectors that did respond to dobutamine stressing compared with those that did not respond. Also, the slope was greatly decreased in sectors that appeared unviable after bypass grafting. As a single MR imaging modality for assessment of unviable sectors, first-pass imaging provided the best sensitivity and specificity results. Contrast enhancement on T1-weighted images was seen in several sectors that had normal wall thickening or that had recovered after surgery; therefore, this approach should not be used as a single method for viability analysis. The combination of cine, stress, and first-pass imaging was the best approach to MR viability analysis in patients with multivessel coronary artery disease. Compared with FDG PET, multimodality MR imaging had good accuracy in the detection of unviable myocardium.

Our finding that low-dose dobutamine cine imaging and systolic wall thickening assessment depicts hibernating and unviable myocardium with good sensitivity and specificity is in agreement with those of earlier articles (3,18,19). Dobutamine

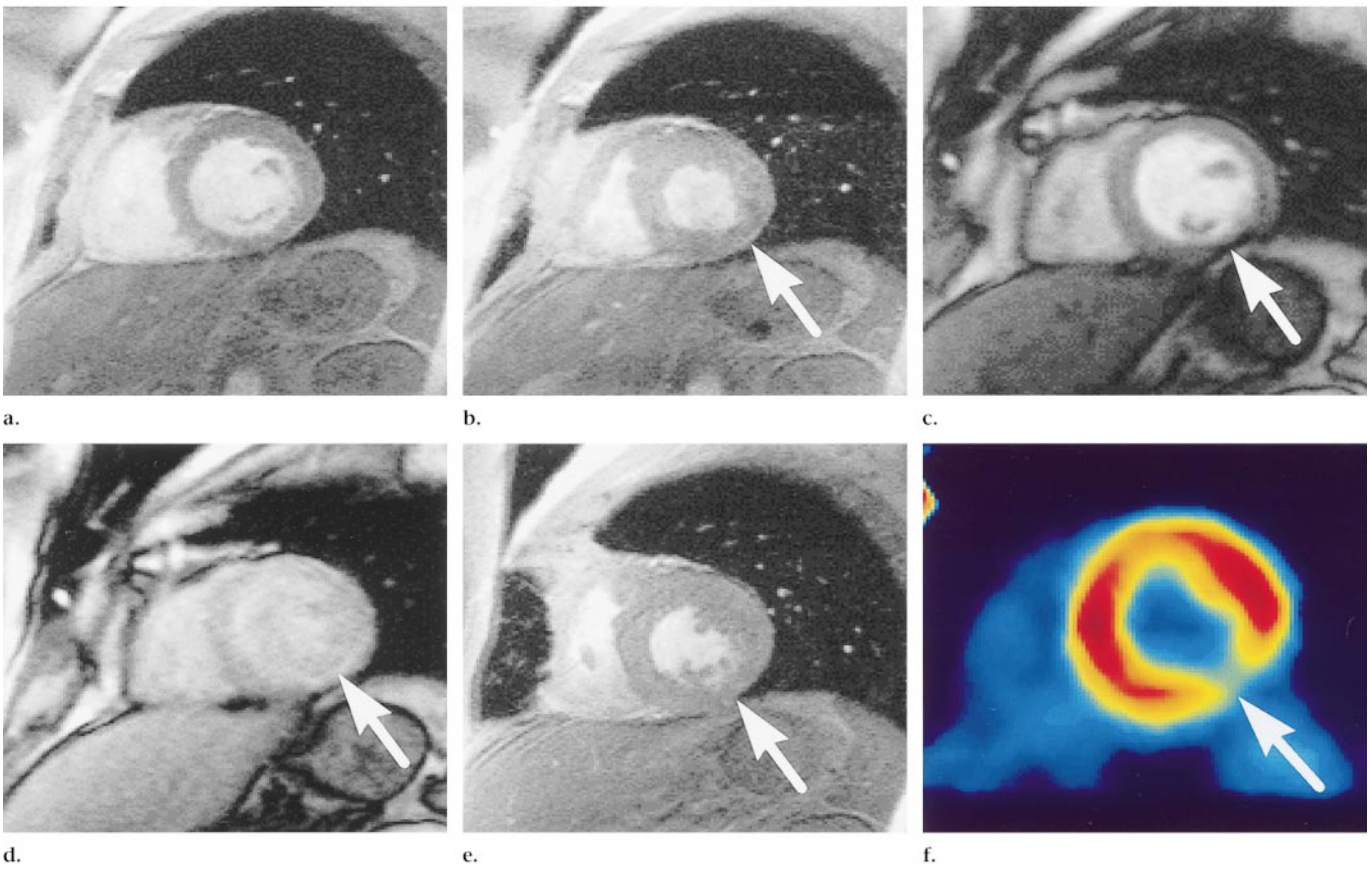

Figure 5. Three MR modalities illustrate posterior unviable myocardium in the left ventricular short-axis section imaged at the level of the papillary muscles. **(a)** End-diastolic cine image. **(b)** End-systolic cine image obtained during dobutamine infusion. Arrow indicates the site of a nonresponding sector on the posterior wall. **(c)** First-pass image obtained during early myocardial contrast enhancement. Arrow indicates the sector with a slower-enhancing posterior wall. **(d)** Arrow indicates the late enhancement in the same sector on this image obtained 5 minutes after contrast agent injection. **(e)** Image of the same left ventricular short-axis section at end systole obtained 6 months after bypass surgery. There is no recovery of systolic wall thickening in the unviable sector. Arrow indicates the site of the nonresponding sector. **(f)** Arrow on the PET image indicates low FDG uptake in the corresponding region. **(a, b, e)** Rest and stress cine images used in the analysis of systolic wall thickening were obtained with an electrocardiographically gated breath-hold sequence (40/4.8; section thickness, 8 mm; field of view, 240 × 320 mm; matrix, 126 × 256). **(c, d)** First-pass MR images and late-enhanced T1-weighted MR images were obtained with an inversion-recovery gradient-echo sequence (3.3/1.4/400; flip angle, 8°; section thickness, 10 mm; field of view, 240 × 320 mm; and matrix, 62 × 128).

infusion with increasing doses does increase the specificity of the wall motion analysis (12), but this method is more time-consuming. On the other hand, first-pass imaging at the single-dose level is fast and requires less image processing and image analysis time.

We found a significant difference in the first-pass enhancement slope of hypokinetic myocardial sectors that did respond to dobutamine when they were compared with the ones that did not and to normal sectors. Similar MR imaging results have not been reported before. We suggest that the difference indicates the dependence of wall motion and perfusion on stress in coronary artery disease. The slope of the enhancement curve is a result of several physiologic factors, such as cardiac output, coronary vasodilatation, and extravasation of low-molecular-weight contrast agent into the myocardial extracellular space (20). The slope is also dependent on the MR imaging parameters and amount of contrast agent used (21). The slope partly reflects regional perfusion, and, according to our findings, wall motion recruitment is tightly dependent on perfusion reserve.

The unviable sectors had a severely decreased first-pass enhancement slope, which distinguished them from viable sectors, with a good sensitivity and specificity. On the other hand, cine imaging showed the hypokinetic sectors, which would recover after treatment. Therefore, the combination of cine and perfusion imaging would be the best MR imaging tool for use in the assessment of both hibernation and viability. MR cine and perfusion imaging with low-dose dobutamine stressing and contrast material injection is safe, fast, and feasible, but image analysis without proper postprocessing tools is time-consuming and is the limiting step for clinical applications.

Contrast enhancement on T1-weighted images alone was the least accurate MR modality in detection of unviable sectors. In earlier studies (22), the size of the hyperintense region was larger than the infarction size assessed with control methods. It has been suggested that the tissue surrounding infarction may be edematous and may, therefore, consist of larger extracellular spaces and an increased distribution volume for the contrast agent (23).

In our patients, the enhancement could have been a result of high signal intensity in subendocardial infarction and the surrounding edema. The response to treatment, therefore, would depend on the transmural extent of the infarction (8),

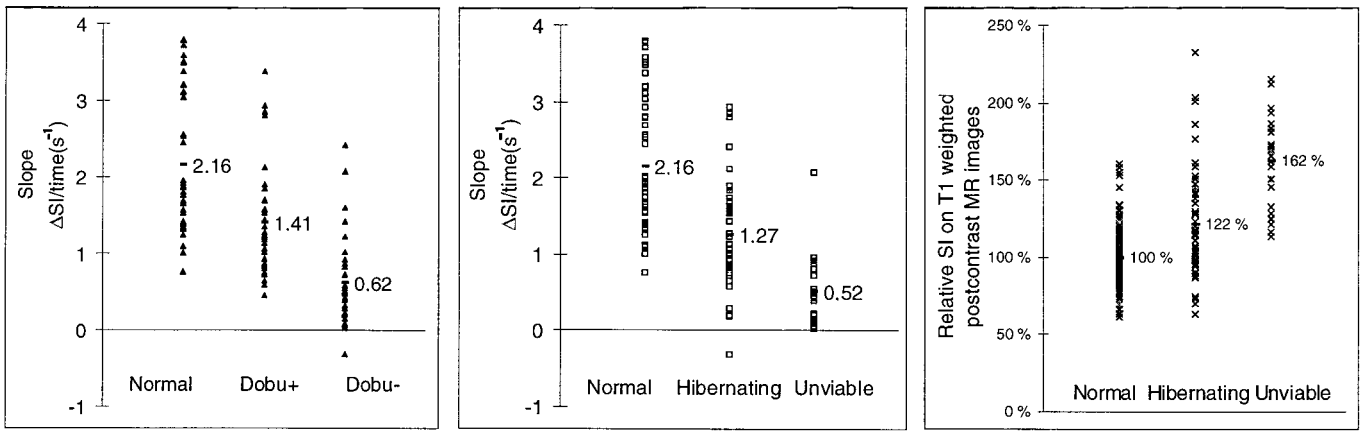

a. **b.** **c.**

Figure 6. Plots show the slope and late enhancement in myocardium during and after the first pass of 0.05 mmol/kg gadopentetate dimeglumine on a series of T1-weighted inversion-recovery gradient-echo (inversion time, 400 msec) images. **(a)** The slope was measured in 43 normal sectors, 43 sectors with decreased (<2 mm) systolic wall thickening at rest that improved by at least 2 mm with low-dose dobutamine infusion (*Dobu+*), and 43 sectors that did not improve (*Dobu−*). The mean in each group is indicated in the plot; the SDs were 0.93, 0.70, and 0.53. **(b)** The slope was measured in 57 normal sectors, 57 sectors that were hypokinetic before but had normal systolic wall thickening after bypass surgery (hibernating), and 29 sectors that were hypokinetic also after surgery (unviable). The mean in each group is indicated in the plot; the SDs were 0.85, 0.73, and 0.43. **(c)** The relative postcontrast enhancement was measured in 57 normal, 57 hibernating, and 29 unviable sectors. The mean in each group is indicated in the plot; the SDs were 18%, 36%, and 30%. *SI* = signal intensity.

which was not assessable with the fast sequence we used. The false-positive sectors on contrast-enhanced images were more often anterior, probably because they were closer to the body array coil. On the other hand, other myocardial diseases such as viral myocarditis (24) and hypertrophic cardiomyopathy (25) have increased signal intensity after contrast agent injection. The high signal intensity on T1-weighted MR images of ischemic myocardium need further study and sector-to-sector comparison with scintigraphic imaging findings.

In the current study, the number of patients was small. Before groups with greater numbers of patients are studied, more automated methods should be developed for quantitative analysis of wall thickening, first-pass imaging, and late enhancement analysis. Because neither angiography nor PET was performed after surgery for control, success in revascularization was not directly assessed. Because first-pass MR imaging with gradient-echo sequences was limited to three left ventricular short-axis sections (5), the entire left ventricular myocardium was not assessed for viability. In the future, faster gradient-echo imaging with inversion recovery (26) or saturation preparation (27), echo-planar sequences (28–30), or a combination of these (31) should be used for whole-heart perfusion and viability imaging.

Author contributions: Study concepts, K.L., P.N., H.H., H.J.A., L.M.V.P.; study design, K.L., H.H., H.J.A., L.M.V.P., L.T.; definition of intellectual content, K.L., P.N., H.H., L.M.V.P., J.K., H.J.A.; literature research, K.L., H.H., T.J.; clinical studies, K.L., P.N., H.H., T.J.; data acquisition, K.L., P.N., H.H., T.J.; data analysis, K.L., T.J., J.K., T.M.; statistical analysis, K.L., T.M.; manuscript preparation, K.L., P.N., H.H., M.A.M., H.J.A.; manuscript editing and review, K.L., P.N., J.K., M.A.M., H.J.A; manuscript final version approval, all authors.

References

1. Baer FM, Voth E, Theissen P, Schicha H, Sechtem U. Gradient-echo magnetic resonance imaging during incremental dobutamine infusion for the localization of coronary artery stenoses. Eur Heart J 1994; 15:218–225.
2. Dendale P, Franken PR, Holman E, et al. Validation of low-dose dobutamine magnetic resonance imaging for assessment of myocardial viability after infarction by serial imaging. Am J Cardiol 1998; 82: 375–377.
3. Baer FM, Voth E, LaRosee K, et al. Comparison of dobutamine transesophageal echocardiography and dobutamine magnetic resonance imaging for detection of residual myocardial viability. Am J Cardiol 1996; 78:415–419.
4. Lima JA, Judd RM, Bazille A, et al. Regional heterogeneity of human myocardial infarcts demonstrated by contrast-enhanced MRI: potential mechanisms. Circulation 1995; 92:1117–1125.
5. Lauerma K, Virtanen KS, Sipila LM, Hekali P, Aronen HJ. Multislice MRI in assessment of myocardial perfusion in patients with single-vessel proximal left anterior descending coronary artery disease before and after revascularization. Circulation 1997; 96:2859–2867.
6. Cullen JH, Horsfield MA, Reek CR, et al. A myocardial perfusion reserve index in humans using first-pass contrast-enhanced magnetic resonance imaging. J Am Coll Cardiol 1999; 33:1386–1394.
7. de Roos A, Doornbos J, van der Wall EE, van Voorthuisen AE. MR imaging of acute myocardial infarction: value of Gd-DTPA. AJR Am J Roentgenol 1988; 150:531–534.
8. Dendale P, Franken PR, Block P, Pratikakis Y, de Roos A. Contrast enhanced and functional magnetic resonance imaging for the detection of viable myocardium after infarction. Am Heart J 1998; 135: 875–880.
9. Rogers WJ Jr, Kramer CM, Geskin G, et al. Early contrast-enhanced MRI predicts late functional recovery after reperfused myocardial infarction. Circulation 1999; 99: 744–750.
10. Ramani K, Judd RM, Holly TA, et al. Contrast magnetic resonance imaging in the assessment of myocardial viability in patients with stable coronary artery disease and left ventricular dysfunction. Circulation 1998; 98:2687–2694.
11. Knuuti MJ, Saraste M, Nuutila P, et al. Myocardial viability: fluorine-18-deoxyglucose positron emission tomography in prediction of wall motion recovery after revascularization. Am Heart J 1994; 127: 785–796.
12. Baer FM, Theissen P, Schneider CA, et al. Dobutamine magnetic resonance imaging predicts contractile recovery of chronically dysfunctional myocardium after successful revascularization. J Am Coll Cardiol 1998; 31:1040–1048.
13. Van Rossum AC, Visser FC, Van Eenige MJ, et al. Value of gadolinium-diethylene-triamine pentaacetic acid dynamics in magnetic resonance imaging of acute myocardial infarction with occluded and reperfused coronary arteries after thrombolysis. Am J Cardiol 1990; 65:845–851.
14. Hamacher K, Coenen HH, Stocklin G. Efficient stereospecific synthesis of no-carri er-added 2-[18F]-fluoro-2-deoxy-D-glucose using aminopolyether supported nucleophilic substitution. J Nucl Med 1986; 27:235–238.

15. Kramer CM. Integrated approach to ischemic heart disease: the one-stop shop. Cardiol Clin 1998; 16:267–276.
16. van der Wall EE, van Rugge FP, Vliegen HW, et al. Ischemic heart disease: value of MR techniques. Int J Card Imaging 1997; 13:179–189.
17. Wilke N, Jerosch-Herold M, Zenovich A, Stillman AE. Magnetic resonance first-pass myocardial perfusion imaging: clinical validation and future applications. J Magn Reson Imaging 1999; 10:676–685.
18. Pennell DJ, Underwood SR, Ell PJ, et al. Dipyridamole magnetic resonance imaging: a comparison with thallium-201 emission tomography. Br Heart J 1990; 64:362–369.
19. Pennell DJ, Underwood SR, Longmore DB. Detection of coronary artery disease using MR imaging with dipyridamole infusion. J Comput Assist Tomogr 1990; 14: 167–170.
20. Arheden H, Saeed M, Higgins CB, et al. Measurement of the distribution volume of gadopentetate dimeglumine at echo-planar MR imaging to quantify myocardial infarction: comparison with ^{99m}Tc-DTPA autoradiography in rats. Radiology 1999; 211:698–708.
21. Canet E, Douek P, Janier M, et al. Influence of bolus volume and dose of gadolinium chelate for first-pass myocardial perfusion MR imaging studies. J Magn Reson Imaging 1995; 5:411–415.
22. Lauerma K, Saeed M, Wendland MF, et al. The use of contrast-enhanced magnetic resonance imaging to define ischemic injury after reperfusion: comparison in normal and hypertrophied hearts. Invest Radiol 1994; 29:527–535.
23. Inoue S, Murakami Y, Ochiai K, et al. The contributory role of interstitial water in Gd-DTPA-enhanced MRI in myocardial infarction. J Magn Reson Imaging 1999; 9:215–219.
24. Friedrich MG, Strohm O, Schulz-Menger J, et al. Contrast media-enhanced magnetic resonance imaging visualizes myocardial changes in the course of viral myocarditis. Circulation 1998; 97:1802–1809.
25. Aso H, Takeda K, Ito T, et al. Assessment of myocardial fibrosis in cardiomyopathic hamsters with gadolinium-DTPA enhanced magnetic resonance imaging. Invest Radiol 1998; 33:22–32.
26. Fritz-Hansen T, Rostrup E, Ring PB, Larsson HB. Quantification of gadolinium-DTPA concentrations for different inversion times using an IR-turbo flash pulse sequence: a study on optimizing multislice perfusion imaging. Magn Reson Imaging 1998; 16:893–899.
27. Penzkofer H, Wintersperger BJ, Knez A, Weber J, Reiser M. Assessment of myocardial perfusion using multisection first-pass MRI and color-coded parameter maps: a comparison to 99mTc Sesta MIBI SPECT and systolic myocardial wall thickening analysis. Magn Reson Imaging 1999; 17:161–170.
28. Edelman RR, Li W. Contrast-enhanced echo-planar MR imaging of myocardial perfusion: preliminary study in humans. Radiology 1994; 190:771–777.
29. Schwitter J, Debatin JF, von Schulthess GK, McKinnon GC. Normal myocardial perfusion assessed with multishot echo-planar imaging. Magn Reson Med 1997; 37:140–147.
30. Debatin JF, McKinnon GC, von Schulthess GK. Technical note: approach to myocardial perfusion with echo planar imaging. Magma 1996; 4:7–11.
31. Ding S, Wolff SD, Epstein FH. Improved coverage in dynamic contrast-enhanced cardiac MRI using interleaved gradient-echo EPI. Magn Reson Med 1998; 39: 514–519.